Table III—Muscle Relaxant Effect of Caracurine V and Its *N*-Oxides in Mice[a]

Compound	Dose, mg/kg	Screen Grip Test
Ia	6	–
	10	++
	13	++++(lethal)
Ib	10	–
	18	++
	25	++(lethal)
Ic	25	–
	40	+++
	60	++++(lethal)

[a] The activity was determined with the screen grip test as it was used in the screening of *Strychnos* plant material (1, 2). The loss of screen grip is rated as follows: ++++, the mouse falls off as the screen is tilted to a 45° angle; +++, the mouse falls off as the screen is tilted to a 90° angle; ++, the mouse falls off as the screen is inverted; and +, the mouse falls off at the first gentle shake.

considerably were C-20 and C-19, 5.04 ppm downfield and 6.44 ppm upfield, respectively. These shifts agree with those observed for strychnine *N*-oxide. The shifts of the signals of the other carbons, although not as large as those mentioned, are also in good agreement for both caracurine V and strychnine (Tables I and II).

The spectrum of Ib obviously results from the addition of the spectra of Ia and Ic. Whether or not the *N*-oxides are artifacts is difficult to say. The *N*-oxides are readily formed, for example, in chloroform solution (3). However, on TLC of a freshly prepared 1% acetic acid in water extract of the stem bark of *S. dolichothyrsa*, the *N*-oxides were observed. The *N*-oxides were tested in the pharmacological screening as described in investigations of African *Strychnos* species (1, 2). Both compounds proved to be less toxic and less active as muscle relaxants than caracurine V (Table III).

REFERENCES

(1) F. Sandberg, E. Lunnell, and K. J. Ryrberg, *Acta Pharm. Suec.*, **6**, 79 (1969).

(2) F. Sandberg, R. Verpoorte, and A. Cronlund, *ibid.*, **8**, 341 (1971).

(3) R. Verpoorte and A. Baerheim Svendsen, *Lloydia*, **39**, 357 (1976).

(4) J. R. Hymon, H. Schmid, P. Karrer, A. Boller, H. Els, P. Fahrni, and A. Fürst, *Helv. Chim. Acta*, **52**, 1564 (1969).

(5) K. Bernauer, F. Berlage, W. v. Philipsborn, H. Schmid, and P. Karrer, *ibid.*, **41**, 2293 (1958).

(6) A. R. Battersby, D. A. Yeowell, L. M. Jackman, H. D. Schroeder, M. Hesse, H. Hiltebrand, W. v. Philipsborn, H. Schmid, and P. Karrer, *Proc. Chem. Soc.*, **1961**, 413.

(7) M. Hesse, "Indolakaloide, Teil 1 und 2, Fortschritte der Massenspektrometrie," vol. 1, Verlag Chemie, Weinheim, West Germany, 1974.

(8) H. Asmis, H. Schmid, and P. Karrer, *Helv. Chim. Acta*, **37**, 1983 (1954).

(9) A. R. Battersby and H. F. Hodson, *J. Chem. Soc.*, **1960**, 736.

(10) H. A. Hiltebrand, Dissertation, Zurich, Switzerland, 1964.

(11) R. Verpoorte, P. J. Hylands, and N. G. Bisset, *Org. Magn. Reson.*, **9**, 567 (1977).

ACKNOWLEDGMENTS

The authors thank Dr. A. J. M. Leeuwenberg, Laboratory of Plant Taxonomy and Plant Geography, Agricultural University, Wageningen, The Netherlands, and Professor Dr. F. Sandberg, Department of Pharmacognosy, Uppsala University, Sweden, for collecting and identifying the plant material.

Light-Scattering Studies on Bile Acid Salts I: Pattern of Self-Association of Sodium Cholate, Sodium Glycocholate, and Sodium Taurocholate in Aqueous Electrolyte Solutions

YUNIK CHANG and JOHN R. CARDINAL ˣ

Received March 4, 1977, from the *College of Pharmacy, University of Utah, Salt Lake City, UT 84112.* Accepted for publication May 10, 1977.

Abstract □ The pattern of association of the trihydroxy bile salts in aqueous electrolyte solutions was investigated utilizing the light-scattering technique. The turbidity of the bile salts sodium cholate, sodium taurocholate, and sodium glycocholate was determined over the concentration range of 0–25 mg/ml at 25°. For sodium cholate, the concentration of the supporting electrolyte was varied from 0.15 to 0.5 *M*. For all bile salts in 0.15 *M* electrolyte, the turbidity was determined in sodium fluoride, sodium chloride, sodium bromide, and sodium iodide. Comparison of the light-scattering data with a monomer–micellar model showed that qualitative agreement was obtained; however, quantitative agreement could not be achieved. Further examination of the data showed that the light-scattering results were in good agreement with a model that includes dimers, trimers, and a higher aggregate containing approximately eight monomeric units.

Keyphrases □ Sodium cholate—pattern of association in aqueous electrolyte solutions, light-scattering study □ Sodium glycocholate—pattern of association in aqueous electrolyte solutions, light-scattering study □ Sodium taurocholate—pattern of association in aqueous electrolyte solutions, light-scattering study □ Association—sodium cholate, glycocholate, and taurocholate, pattern in aqueous electrolyte solutions, light-scattering study □ Light scattering—study of pattern of association of sodium cholate, glycocholate, and taurocholate in aqueous electrolyte solutions □ Bile acid salts—pattern of association in aqueous electrolyte solutions, light-scattering study

The mechanism by which bile salts solubilize various solutes such as steroids, fat-soluble vitamins, and drugs has often been described following the model for detergent micelles (1). In this model, it is assumed that a reversible equilibrium exists between monomeric species and micelles. The polydispersity of the micelle is assumed to be quite small. The micelle size is dependent on the nature of the bile salt, *i.e.*, the number of hydroxyl groups and conjugation, as well as on temperature, pH, ionic strength, *etc.* (2).

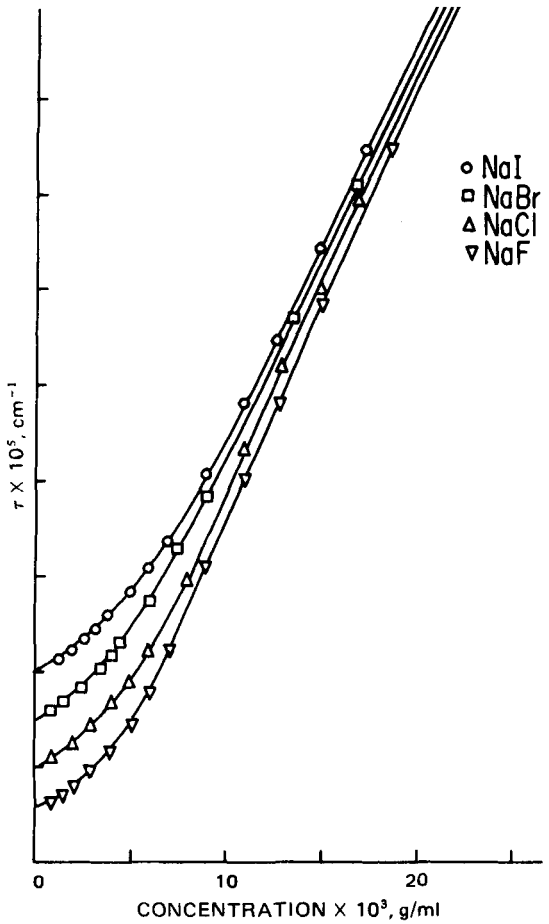

Figure 1—*Plots of the turbidity, τ,* versus *concentration of sodium cholate in 0.15* M *sodium halides. Each division on the ordinate represents 5 × 10^{-5} cm^{-1}. The intercepts representing the turbidity of the solvent are: sodium iodide, 5.98 × 10^{-5} cm^{-1}; sodium bromide, 5.32 × 10^{-5} cm^{-1}; sodium chloride, 5.07 × 10^{-5} cm^{-1}; and sodium fluoride, 4.85 × 10^{-5} cm^{-1}.*

In contrast, other studies (3–6) suggested that the self-association of the bile salts occurs in a stepwise fashion and that various concentration limits for the association process can be defined. The concentration limits are approximately the same for all trihydroxy bile salts, while different limits exist for all dihydroxy bile salts. These concentration limits define regions over which the association process remains relatively constant. Discrete changes in both the nature of the association and the aggregation number are thought to occur at these concentration limits.

Recently, Mukerjee and Cardinal (7) investigated the self-association of the bile salt sodium cholate in water in the absence of added electrolytes. An attempt was made to explain the variation in total naphthalene solubility as a function of the sodium cholate concentration on the basis of various self-association models. Comparison of the sodium cholate solubilization data with solubilization data from a typical micelle-forming system, sodium decanesulfonate, showed clearly that the solubilization process for sodium cholate does not resemble a micellar system. In addition, the solubility data were inconsistent with the reported concentration limit model (3–6).

Mukerjee and Cardinal (7) also concluded that the solubilization data were consistent with a model that requires the existence of dimers and some higher oligomers. More definite conclusions could not be reached because of uncertainties of the assumed models. A similar conclusion about the concentration limit model was also reached by Vitello (8) based on the analysis of light-scattering data.

The purpose of the present study was to examine the self-association pattern of the bile salts. The variation of the light scattered as a function of concentration was obtained for sodium cholate, sodium glycocholate, and sodium taurocholate in 0.15 *M* sodium halides. The effect of electrolyte concentration was determined for sodium cholate. The light-scattering curves were examined in terms of various association models.

EXPERIMENTAL

Materials—Cholic acid[1] was recrystallized according to the method of Hofmann (9). Taurocholic acid and glycocholic acid were synthesized from cholic acid according to the method of Lack *et al.* (10). All bile acids were found to be free of other bile acids by TLC (100-μg spot). In addition, the conjugated acids were found to be free of glycine ethyl ester or taurine by TLC.

In all cases, the sodium salts were obtained by titration of the free acid with sodium hydroxide to pH 10.0 in water. The solid salts were obtained by solvent removal in a flash evaporator followed by overnight drying in a vacuum oven at 45°. All inorganic salts were used as received, except sodium fluoride which was recrystallized from water.

All water was obtained as follows: laboratory distilled water was passed through an ion-exchange column[2], distilled twice from an all-glass still, and stored in all-glass containers.

Apparatus—Light-scattering measurements were made with a light-scattering photometer[3] using the small dissymmetry cell[4] centered in the light beam with four polymer pieces of equal width. These pieces were utilized to align the cell in the light beam by the scored markings on the cell table supplied with the instrument.

Refractive index measurements[5] also were obtained. Temperature control[6] of the refractometer was maintained at 25 ± 0.2°. The pH measurements were made with a digital pH meter[7].

Light-Scattering Measurements—Solutions for the light-scattering measurements were made either by dilution or by direct weighing of the required quantities. All dilutions were made from initial stock solutions adjusted to pH 10.0.

The usual methods employed for the removal of particulate matter from solutions for the light-scattering measurements, such as repeat filtration or ultracentrifugation, were inadequate for this investigation. However, the following procedure yielded particulate-free solutions. A syringe was filled with 50 ml of the solution for measurement, approximately 25 ml of this solution was filtered (0.22-μm filter[8] pore diameter) and saved for future use, and, without removal of the applied pressure, the final portion of the solution was filtered directly into the light-scattering cell. The scattering cell had been cleaned previously in an apparatus of the type designed by Schipmann and Farber (11).

With this technique, scattering ratios reproducible within the ability to read the galvanometer deflection were obtained. This reproducibility was found for both repeat measurements of the same sample and for successive portions of a sample of a given concentration.

The light-scattering measurements were obtained at 436 nm at room temperature, which was close to 25°. The instrument was calibrated routinely with water according to the method of Huisman (12). The value of 4.79 × 10^{-5} cm^{-1} was accepted for the turbidity of water (12). As a check on this calibration method, the turbidity of benzene and carbon tetrachloride was measured using the instrument constant from the described procedure. A value of 2.50 × 10^{-4} cm^{-1} was found for carbon tetrachloride, and 7.71 × 10^{-4} cm^{-1} was obtained for benzene. These values compare very well with those of Coumou (13), who reported 2.48

[1] J. T. Baker Chemical Co., Phillipsburg, N.J.
[2] Model LD-2a, Corning Glass Works, Corning, N.Y.
[3] Brice-Phoenix model BP-2000, Virtis Co., Gardiner, N.Y.
[4] Catalog No. D105, Virtis Co., Gardiner, N.Y.
[5] Brice-Phoenix differential refractometer, model BP-2000-V, Virtis Co., Gardiner, N.Y.
[6] Lauda circulating water bath, model K2-R, Brinkmann Instruments, Westbury, N.Y.
[7] Model 110, Corning Glass Works, Corning, N.Y.
[8] Millipore Filter Corp., Bedford, Mass.

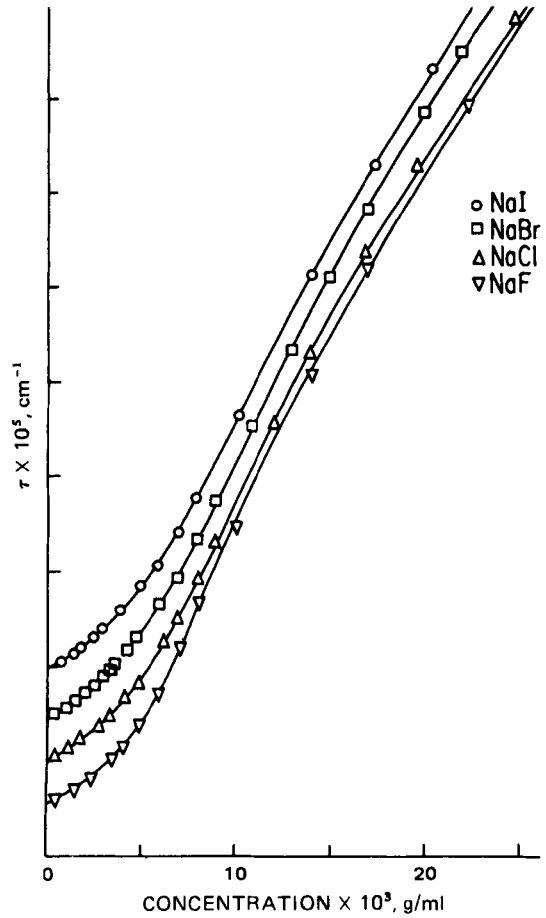

Figure 2—*Plots of the turbidity, τ,* versus *concentration of sodium taurocholate in 0.15* M *sodium halides. The units of the ordinate and the intercepts are the same as in Fig. 1.*

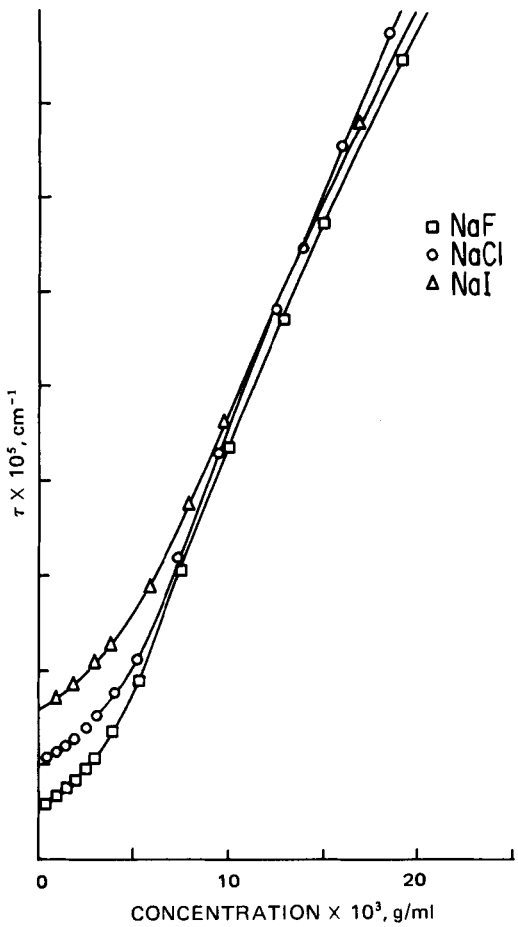

Figure 3—*Plots of the turbidity, τ,* versus *concentration of sodium glycocholate in 0.15* M *sodium halides. The units of the ordinate and the intercepts are the same as in Fig. 1.*

$\times 10^{-4}$ cm^{-1} for carbon tetrachloride and 7.64 $\times 10^{-4}$ cm^{-1} for benzene.

All solutions were checked for dissymmetry, and only solutions showing a dissymmetry of less than 1.03 were utilized. Depolarization and fluorescence of the scattered light were negligible.

RESULTS

The turbidity, τ (in centimeters^{-1}), as a function of the bile salt concentration (in grams per milliliter) for various trihydroxy bile salts in 0.15 *M* sodium halides is shown in Figs. 1–3. Figure 4 is a similar plot for sodium cholate in 0.3 and 0.5 *M* sodium chloride. The refractive increments, *dn/dc*, at a constant electrolyte concentration for the various systems studied are given in Table I. A comparison of the *dn/dc* values reported by previous workers is also included.

DISCUSSION

The results shown in Figs. 1–4 are in qualitative agreement with those found previously (2, 4, 8, 14, 15). The turbidity increased slowly at low concentrations, followed by a relatively rapid increase at higher concentrations. This relatively rapid increase is usually attributed to micelle formation. However, no "kinks" or "breaks" appear in the plots. Thus, as pointed out by Vitello (8), the light-scattering data appear to be inconsistent with the concentration limit model of Ekwall *et al.* (3) and Fontell (4–6).

In the following sections, these data will be compared with the monomer–micelle equilibrium model. It will be shown that these data are in relatively poor agreement with this model. A new model will be described for the association process which yields substantially better agreement with the experimental results.

Monomer–Micelle Equilibrium Model—The usual method for investigating the self-association of the bile salts by light scattering has followed the techniques outlined by Debye (16). This method assumes the existence of a critical micelle concentration (CMC). The concentration of the monomer unit is assumed to increase linearly with concentration below this value and to remain nearly equal to this value above the CMC. These assumptions permitted Debye to derive the following equations, which permit the determination of the molecular weight, M, and the second virial coefficient, B, for the micelle:

$$\frac{H(c - c_0)}{(\tau - \tau_0)} = \frac{1}{M} + 2B(c - c_0) \qquad \text{(Eq. 1}a\text{)}$$

where:

$$H = \frac{32\pi^3 n^2 (dn/dc)^2}{3\lambda_0^4 N_A} \qquad \text{(Eq. 1}b\text{)}$$

and c represents the total concentration (in grams per milliliter), τ represents the total turbidity at concentration c, c_0 and τ_0 are the respective

Table I—Summary of Refractive Index Increments for the Trihydroxy Bile Salts

Solvent	*dn/dc* at 436 nm, ml/g: Sodium Cholate, Present Work	Sodium Taurocholate, Present Work	Sodium Taurocholate, Ref. 8	Sodium Glycocholate, Present Work
0.15 *M* Sodium fluoride	0.191	0.167	0.168	0.189
0.15 *M* Sodium chloride	0.193	0.166	0.172	0.184
0.15 *M* Sodium bromide	0.194	0.164	0.172	—
0.15 *M* Sodium iodide	0.193	0.173	0.165	0.189
0.3 *M* Sodium chloride	0.196	—	—	—
0.5 *M* Sodium chloride	0.197[a]	—	—	—

[a] Vitello (8) found 0.186.

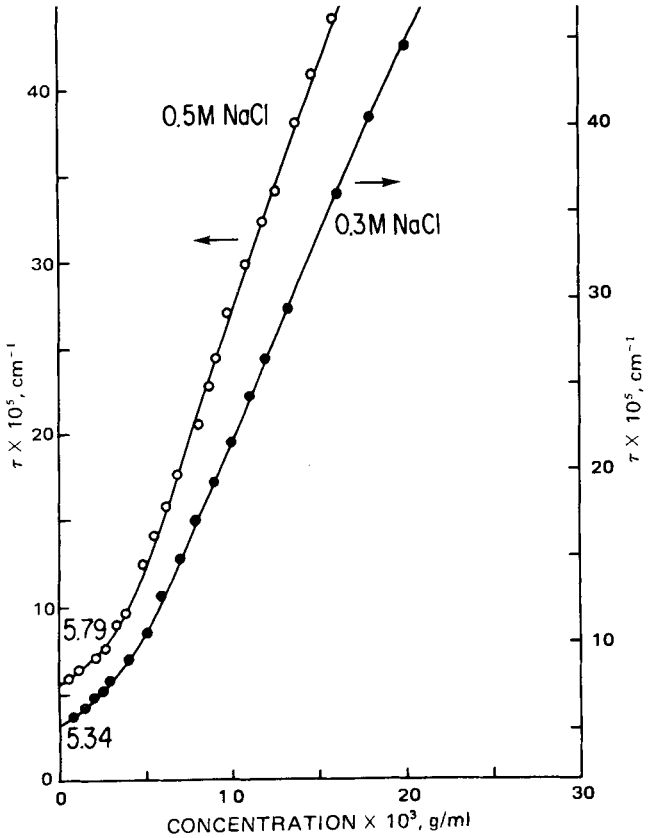

Figure 4—*Plots of the turbidity, τ, as a function of the concentration of sodium cholate in 0.3 and 0.5* M *sodium chloride.*

values at the CMC, n is the refractive index of the solution, dn/dc is the refractive increment at a constant concentration of the supporting electrolyte, λ_0 is the wavelength of light in vacuum, and N_A is Avogadro's number. The micelle molecular weight and the second virial coefficient are obtained from the intercept and slope of a plot of $H(\Delta c/\Delta\tau)$ *versus* Δc.

The equation of Debye is valid for a two-component system containing solvent and uncharged colloidal particles. However, in a three-component system containing, for example, solvent, salt, and charged colloidal particles, the approach of Debye is not totally applicable. Vrij and Overbeek (17) showed that the problem arises from the negative adsorption of the salt on the colloidal particles and that the true molecular weight of the aggregate and the true second virial coefficient can be obtained from the following equations:

$$\frac{H'\,\Delta c}{\Delta\tau} = \frac{1}{\mathrm{M}} + 2B\,\Delta c \qquad \text{(Eq. 2}a\text{)}$$

where:

$$H' = \frac{H(dn/dc_1)^2\mu_s}{(dn/dc_1)^2c_2} \qquad \text{(Eq. 2}b\text{)}$$

where $(dn/dc_1)c_2$ is the same as the refractive increment used in Eq. 1*b* and $(dn/dc_1)\mu_s$ is the refractive increment for the colloid at a constant chemical potential of the supporting electrolyte. For micellar systems, the monomeric surfactant ions are assumed to be a part of the supporting electrolyte (12). The value of $(dn/dc_1)\mu_s$ can be obtained from:

$$\left(\frac{dn}{dc_1}\right)_{\mu_s} = \left(\frac{dn}{dc_1}\right)_{c_2}\left[1 + \frac{(dn/dc_2)c_1}{(dn/dc_1)c_2}\left(\frac{dc_2}{dc_1}\right)_{\mu_s}\right] \qquad \text{(Eq. 3)}$$

where $(dn/dc_2)c_1$ is the refractive increment of the supporting electrolyte and $(dc_2/dc_1)\mu_s$ represents the negative adsorption of the supporting electrolyte on the micellar aggregate. Vrij and Overbeek (17) showed that this latter quantity can be obtained from:

$$\mathrm{M_1}^* = \mathrm{M_1}\left[1 + \frac{(dn/dc_2)c_1}{(dn/dc_1)c_2}\left(\frac{dc_2}{dc_1}\right)_{\mu_s}\right]^2 \qquad \text{(Eq. 4)}$$

where $\mathrm{M_1}^*$ represents the apparent molecular weight of the micelle obtained from Eq. 1*a*. The true molecular weight of the micelle $\mathrm{M_1}$ can be obtained from the intercept of a plot of $\mathrm{M_1}^*$ *versus* $(dn/dc_2)c_1$ according to Eq. 4. This procedure assumes that the negative adsorption is independent of the nature of the co-ion found in solution (12). The usual procedure for obtaining $\mathrm{M_1}$ is to determine $\mathrm{M_1}^*$ from Eq. 1*a* for various halides at a given electrolyte concentration and to plot according to Eq. 4.

Table II—CMC Values for Sodium Taurocholate in 0.15 *M* Sodium Halides at 25°

Salt	CMC, g/ml		
	Present Work	Ref. 8	Ref. 18[a]
Sodium fluoride	0.0040	0.0045	—
Sodium chloride	0.0048	0.0039	0.00141
Sodium bromide	0.0044	0.0045	—
Sodium iodide	0.0047	0.0040	—

[a] At 20°.

Huisman (12) utilized the approach outlined to investigate the micelle molecular weights of sodium alkyl sulfates as a function of electrolyte concentration and showed that the neglect of the negative adsorption effect as in the Debye approach leads to micelle molecular weights that are too low. In addition, Huisman showed (12) that excellent agreement between experimental results and calculated curves can be obtained from Eq. 2*a* and from the following equation, which gives the concentrations of the monomer and micelle:

$$\beta = \frac{f_q c_q}{f_1{}^q c_1{}^q} \qquad \text{(Eq. 5)}$$

where f_q is the activity coefficient of the micelle (assumed to be unity), c_q is the concentration of micelles, f_1 is the activity coefficient of the monomer, c_1 is the monomer concentration, q is the aggregation number, and β is the equilibrium constant. This equation neglects counterion effects on the equilibrium process; however, for the systems investigated here, the concentration of the counterion is large and effectively constant. Therefore, this equation should hold for the systems of interest.

In the present study, the necessary data for application of Eqs. 2*a*–5 to the systems of sodium cholate, sodium taurocholate, and sodium glycocholate in 0.15 *M* sodium halides were obtained. However, for comparison of these systems with the monomer–micelle model, only data for sodium taurocholate will be utilized; the results for the other systems are qualitatively the same.

As discussed previously (7), the value obtained for the CMC in bile salt solutions cannot be defined precisely but largely depends on the range of concentrations utilized in the extrapolation. For example, these investigators (7) found CMC values that differ by almost a factor of two from sodium cholate solubilization data, depending on the range of concentrations used in the extrapolation. This same phenomenon was found for the light-scattering data. This result is due to the high degree of curvature found in the CMC region.

However, if the extrapolations are made using only the lowest concentrations and the concentration range greater than about 8×10^{-3} g/ml, then a fairly consistent set of CMC values for sodium taurocholate can be obtained from the data shown in Fig. 2. These values are given in Table II, along with values obtained by other workers for the same systems. The results obtained in this work are slightly higher than those of Vitello (8) but are within the error of the extrapolation.

With the values obtained for the CMC shown in Table II, the apparent aggregation number and the apparent second virial coefficient for sodium taurocholate micelles were obtained according to Eq. 1*a*. These values are shown in Table III, together with a comparison of values obtained by previous workers. The results obtained in the present study appear to be consistent with those obtained previously.

To determine the extent to which the monomer–micelle model represents the nature of the association of sodium taurocholate, a comparison

Table III—Summary of Aggregation Numbers and Second Virial Coefficients for Sodium Taurocholate Micelles in 0.15 *M* Sodium Halides at 25°

Salt	Aggregation Number		$B \times 10^4$, ml mole/g^2
	Present Work	Ref. 8	
Sodium fluoride	6.0	7.6	0.62
Sodium chloride	5.7	7.1, 4.6[a], 7[b]	0.83
Sodium bromide	5.6	6.7	0.81
Sodium iodide	4.7	5.4	0.75

[a] Reference 2. [b] Reference 19.

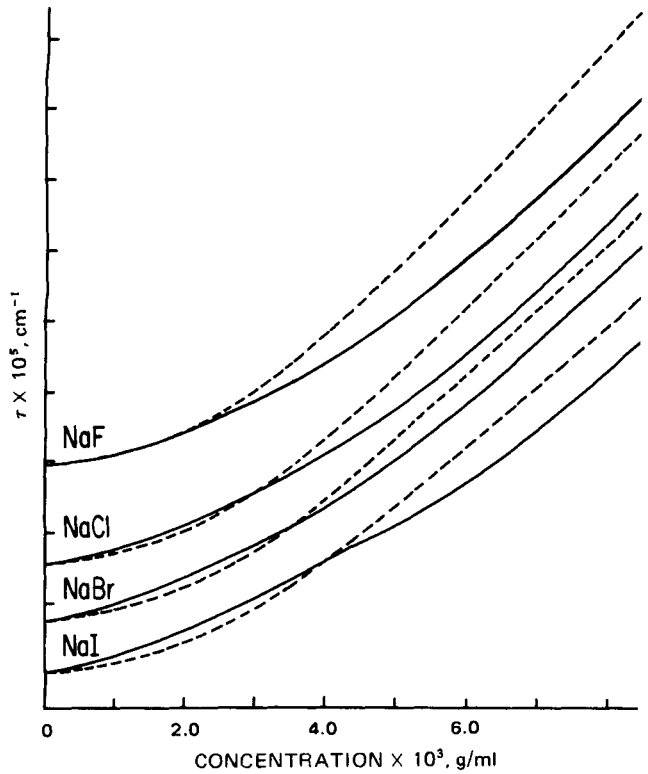

Figure 5—*Comparison of the calculated turbidity (- - -) for sodium taurocholate based on the monomer–micellar model with the experimental curve (—) in the low concentration region. Each division on the ordinate represents* 2×10^{-5} *cm*$^{-1}$.

between the experimental curves and those obtained by calculation according to Eqs. 2*a*–5 was made. The true micelle molecular weight was 3490 according to Eq. 4. This value corresponds to a true aggregation number of 6.49. With the value of $(dc_2/dc_1)\mu_s$ obtained from the plot of Eq. 4, the value of H' for each of the four salt systems was found from Eqs. 2*b* and 3. For the monomer–micelle model, the total concentration of the bile salt is given by:

$$C_T = C_{mon} + q\beta[C_{mon}]^q \qquad \text{(Eq. 6)}$$

where C_{mon} is the concentration of the monomer unit in molar units, q is the aggregation number, and β is the equilibrium constant. The total turbidity for the system is given by:

$$\tau_T = \tau_0 + \tau_{mon} + \tau_{mic} \qquad \text{(Eq. 7)}$$

where τ_0 is the total turbidity of the solvent (water plus electrolyte), τ_{mon} is the turbidity due to the monomer, and τ_{mic} is the turbidity due to the micelle. To calculate the total turbidity at any concentration, C_T, it is only necessary to combine the values obtained from Eqs. 2*a*–6 together with the experimentally measured value for τ_0. The value of β is obtained by fitting one experimental curve. Then all of the remaining values for the various halides can be calculated. It is assumed that the activity coefficient of the monomer is constant in 0.15 *M* sodium halides.

Figure 5 gives a comparison of the experimental and calculated curves for the various halides at a low concentration. Figure 6 shows the comparison for the entire concentration range from 0 to 25×10^{-3} g/ml. In this calculation, 6.5 was taken as the aggregation number, 7.5×10^{-4} mole ml/g^2 was used for the second virial coefficient (average value of those shown in Table III), and 1.23×10^{11} was found for the association constant. Therefore, the only variable among the four different halide systems was the value of H', which was obtained as outlined above.

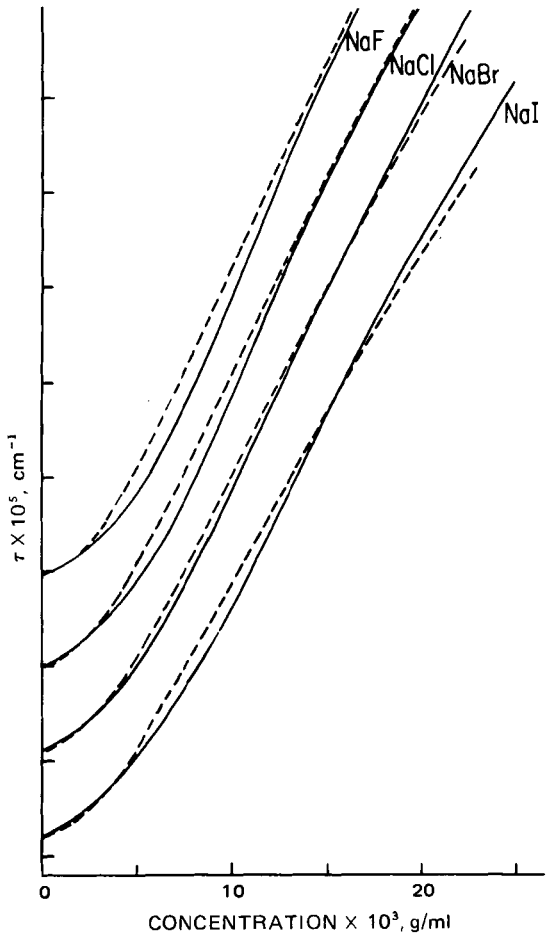

Figure 6—*Comparison of the calculated turbidity (- - -) for sodium taurocholate with the experimental values (—) for the entire concentration range from 0 to* 25×10^{-3} *g/ml. The units of the ordinate are the same as in Fig. 1.*

From Figs. 5 and 6, it can be seen that at very low concentrations, the calculated curves fall below the experimental curves; at intermediate concentrations, the calculated curves are substantially above the experimental values. If other consistent values are chosen for B, q, and β, the regions of disagreement between the calculated and experimental curves will vary. However, it was not possible to obtain a consistent set of parameters that would reproduce the experimental curve assuming the existence of only monomers and a higher oligomer.

This type of comparison between the experimental results and the calculated curves was also made for sodium cholate and sodium glycocholate. A similar trend was obtained in these systems.

Based on these results, it is concluded that qualitative agreement between the calculated curves and the experimental values can be obtained with the monomer–micelle model. That is, the shape of the calculated

Table IV—Equilibrium Constants, Second Virial Coefficients, Molecular Weights, and Aggregation Numbers for Sodium Cholate in 0.15 *M* Sodium Halides

Salt	K_2, liters/mole	K_3, liters/mole	Second Virial Coefficient, ml mole/g^2	Molecular Weight	Aggregation Number
Sodium fluoride	8.5	300	4.0×10^{-3}	3170	7.4
Sodium chloride	6.9	260	5.3×10^{-3}	3110	7.2
Sodium bromide	7.0	300	3.5×10^{-3}	2600	6.0
Sodium iodide	6.5	320	4.6×10^{-3}	2780	6.5
Average or extrapolated values	7.2	293	4.38×10^{-3}	3240	7.63

Table V—Equilibrium Constants, Second Virial Coefficients, Molecular Weights, and Aggregation Numbers for Sodium Taurocholate in 0.15 *M* Sodium Halides

Salt	K_2, liters/mole	K_3, liters/mole	Second Virial Coefficient, ml mole/g^2	Molecular Weight	Aggregation Number
Sodium fluoride	20	240	1.2×10^{-3}	3950	7.4
Sodium chloride	35	310	1.2×10^{-3}	3620	6.7
Sodium bromide	33	350	1.3×10^{-3}	3370	6.3
Sodium iodide	31	240	1.2×10^{-3}	3200	5.9
Average or extrapolated values	30	290	1.22×10^{-3}	4120	7.67

Table VI—Equilibrium Constants, Second Virial Coefficients, Molecular Weights, and Aggregation Numbers for Sodium Glycocholate in 0.15 *M* Sodium Halides

Salt	K_2, liters/mole	K_3, liters/mole	Second Virial Coefficient, ml mole/g^2	Molecular Weight	Aggregation Number
Sodium fluoride	34	240	2.4×10^{-3}	3900	8.0
Sodium chloride	34	200	2.2×10^{-3}	3490	7.2
Sodium iodide	35	190	2.4×10^{-3}	3370	6.9
Average or extrapolated values	34.2	210	2.32×10^{-3}	3930	8.05

curves follows the same trend as the experimental values in that the turbidity increases slowly at low concentrations, followed by a region with curvature, and then increases nearly linearly with concentration. However, with this model, it is not possible to obtain calculated curves that reproduce the experimental results quantitatively throughout the concentration range investigated. This result can only mean that the monomer–micelle equilibrium model does not adequately describe the self-association of the trihydroxy bile salts in aqueous solution. The conclusion is similar to that reached in earlier work based on the solubilization of naphthalene by sodium cholate (7).

Stepwise Association Models—Attwood and Udeala (21, 22) showed that the method of Steiner (20) can be utilized to differentiate between various association models for the self-association of various antihistamines by light-scattering techniques. In the present study, the method of Steiner was applied to gain insight into the self-association of the bile salts.

In this model, aggregate growth is assumed to occur by stepwise addition of monomers to existing monomers or aggregates. The simplest of such schemes is dimerization, which can be represented by:

$$2b_1 \overset{K_2}{\rightleftarrows} b_2$$

Scheme I

and:

$$K_2 = \frac{b_2}{b_1^2} \qquad \text{(Eq. 8)}$$

where b_1 is the monomer concentration, b_2 is the dimer concentration, and K_2 is the association constant for dimerization. Further steps in this process can be written as:

$$b_2 + b_1 \overset{K_3}{\rightleftarrows} b_3$$

$$b_3 + b_1 \overset{K_4}{\rightleftarrows} b_4$$

$$b_{q-1} + b_1 \overset{K_q}{\rightleftarrows} b_q$$

Scheme II

The total equivalent concentration is given by:

$$C_T = b_1 + 2K_2[b_1]^2 + 3K_2K_3[b_1]^3 + \cdots q \prod_2^q K_q[b_1]^q \qquad \text{(Eq. 9a)}$$

$$C_T = \sum q b_q \qquad \text{(Eq. 9b)}$$

The various association constants K_2, K_3, *etc.*, can be obtained by the method developed by Steiner (20). According to this method of analysis, the weight-average molecular weight of the aggregates is related to weight concentration, c (grams per milliliter), by:

$$M/M_w = 1 + d \ln x/d \ln c \qquad \text{(Eq. 10)}$$

where M is the molecular weight of the monomer and x is the weight

Table VII—Equilibrium Constants, Second Virial Coefficients, Association Constants, and Aggregation Numbers for Sodium Cholate in Various Concentrations of Sodium Chloride

Concentration of Sodium Chloride, mole/liter	K_2, liters/mole	K_3, liters/mole	β_q	Second Virial Coefficient, ml mole/g^2	Aggregation Number
0.15	6.9	206	5.2×10^{11}	5.4×10^{-3}	7.2
0.30	16	400	8.3×10^{11}	1.4×10^{-3}	6.4
0.50	10	330	7.2×10^{11}	2×10^{-3}	8.9

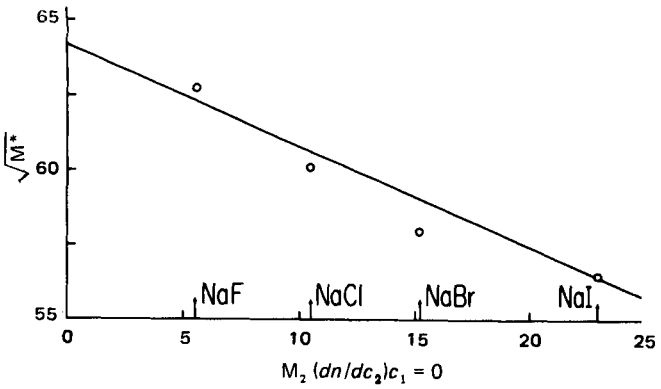

Figure 7—*Plot for the determination of true molecular weight of the high aggregate for sodium taurocholate.*

fraction of species existing as monomeric units. The value of M_w is obtained by application of the equation:

$$\frac{Hc}{\Delta\tau} = \frac{1}{M_w} + 2Bc \qquad \text{(Eq. 11)}$$

in which it is assumed that the second virial coefficient can be neglected. The parameter $\Delta\tau$ represents the excess turbidity of the solution over the solvent. The weight fraction of the monomer can be obtained by graphical integration according to:

$$\ln x = \int_0^c [(M/M_w) - 1] d \ln c \qquad \text{(Eq. 12)}$$

The equilibrium constants can be obtained from:

$$\frac{[(M_w/xM) - 1]}{(xc/M)} = 4K_2 + 9K_2K_3(xc/M) \cdots + q^2 \prod_2^q K_q(xc/M)^{q-2} \qquad \text{(Eq. 13)}$$

where K_2 is obtained from the intercept and K_3 is obtained from the slope of the plot of the data according to Eq. 13. Higher association constants can be obtained by successive application of this equation.

Application of Eq. 13 to the light-scattering data for the bile salts sodium cholate, sodium taurocholate, and sodium glycocholate in 0.15 *M* sodium halides leads to a consistent set of values for K_2 and K_3 (Tables IV–VI). For each bile salt in the various halides, the values of K_2 and K_3

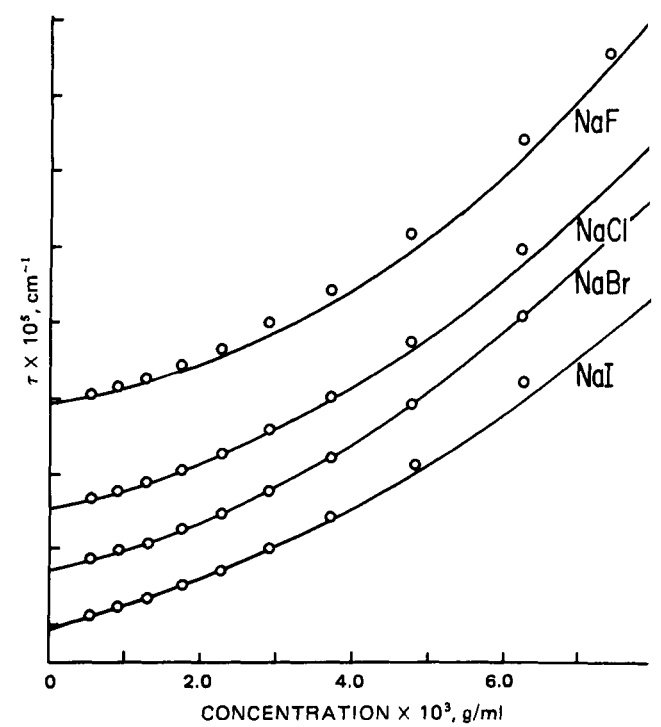

Figure 8—*Comparison of the experimental curves (—) for sodium taurocholate with the calculated values (O) based on the model depicted by Eq. 14b. The units of the ordinate are the same as in Fig. 5.*

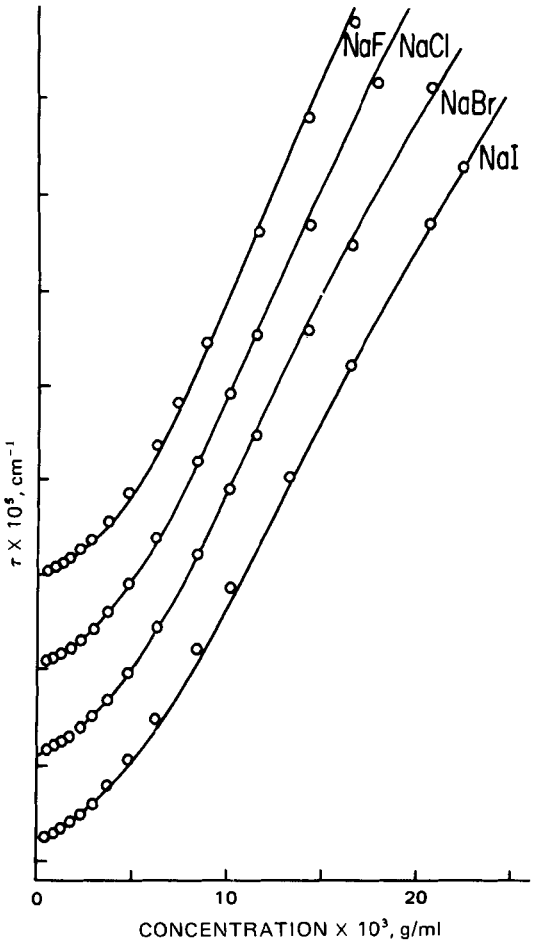

Figure 9—*Comparison of the experimental curves (—) for sodium taurocholate with the calculated values (O) based on the model depicted by Eq. 14b for the entire concentration range from 0 to 25 × 10^{-3} g/ml. The units of the ordinate are the same as in Fig. 1.*

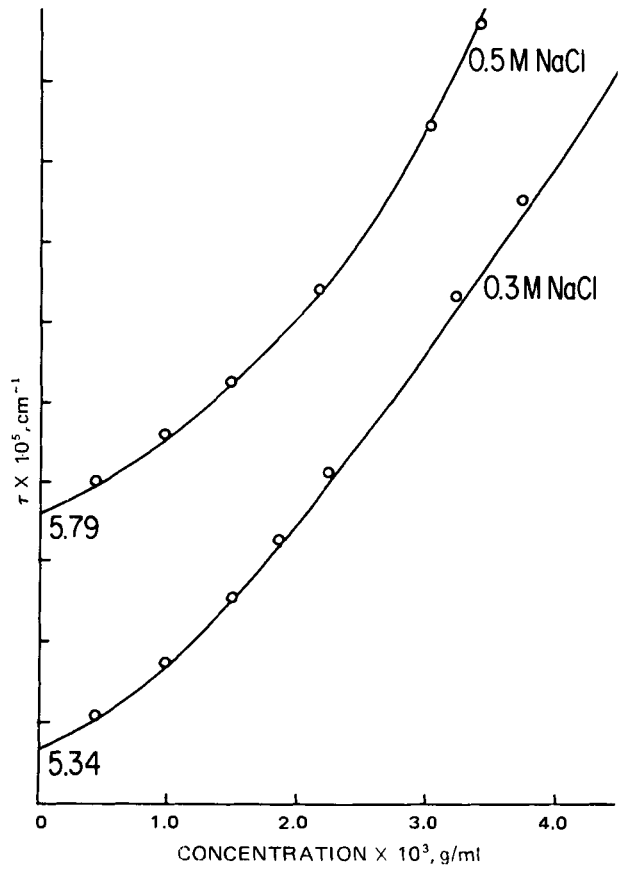

Figure 10—*Comparison of the experimental curves (—) for sodium cholate in 0.3 and 0.5 M sodium chloride with the calculated values (O) based on the stepwise association model depicted by Eq. 14b. Each division of the ordinate represents 1 × 10^{-5} cm^{-1}.*

are nearly the same. However, when Eq. 13 was extended to obtain a value for K_4, the initial slopes of these plots were always nearly zero. At higher values of xc/M, the plots tend to increase rapidly. This result was interpreted to indicate that the value of K_4 must be small relative to the lower association constants and, therefore, that the stability of the tetramer is small with respect to that of the dimer and trimer. On the other hand, the rapid increase of the plots at higher values of xc/M suggests that aggregates larger than the trimer must exist in solution.

To determine the size and association constants for these higher aggregates, the procedure as outlined is not applicable since reliable estimates of K_4, K_5, *etc.*, cannot be obtained. However, based on the qualitative agreement between the experimental results and the monomer–micellar model discussed previously, as well as the results mentioned here, it seems reasonable to assume that higher aggregates must exist. This assumption suggests that the total equivalent concentration, C_T, for the trihydroxy bile salts may follow a model given by:

$$C_T = b_1 + 2b_2 + 3b_3 + qb_q \qquad \text{(Eq. 14a)}$$

$$C_T = b_1 + 2K_2b_1^2 + 3K_2K_3b_1^3 + q\beta_q b_1^q \qquad \text{(Eq. 14b)}$$

where b_1, b_2, b_3, and b_q represent the concentrations of monomer, dimer, trimer, and higher aggregate at the total concentration C_T, respectively; q is the average aggregation number of the higher aggregate; and β_q is the average overall association constant for the formation of b_q as defined by Eq. 9a. The concentration of intermediate-sized aggregates is assumed to be small.

To test this model against the experimental results, it was necessary to develop a method by which the average size of this higher aggregate could be determined. A somewhat similar question was addressed previously by Mysels and Princen (23) in their considerations of light scattering by sodium lauryl sulfate. For this system, the monomeric ions of sodium lauryl sulfate were thought to exist in equilibrium with lauryl sulfate dimers below the CMC (24). To take this effect into account, Mysels and Princen utilized the Debye treatment to obtain the apparent micelle molecular weight. However, it was assumed that the turbidity at the CMC could be calculated to be that due to the solvent, monomers, and dimers.

In the analysis of the light-scattering data for the bile salts according to the model depicted by Eq. 14*b*, a procedure similar to that of Mysels and Princen (23) was followed. However, because of the expected low aggregation number of the higher aggregate, certain alternatives were adopted. An assumption inherent in the law of mass action when applied to micellar systems (Eq. 5) is that the monomer activity must increase with an increase in total concentration (25). This increase in activity is related to the weight average degree of association and would be expected to be significant for aggregates as small as 7–8-mers (25).

In the present systems, this increase in activity can be obtained directly from application of Eq. 12, assuming that the activity coefficients are constant. Therefore, at any C_T, the concentration of monomer is known, allowing calculation of the total turbidity due to monomers, dimers, and trimers at that C_T according to Eq. 11. In the same way, the total concentration of these species at any given C_T can be calculated. Thus, the apparent molecular weight of the higher aggregate can be obtained from:

$$\frac{H(c - c_0')}{(\tau - \tau_0')} = \frac{1}{M} + 2B(c - c_0') \qquad \text{(Eq. 15)}$$

where $c_0' = b_1 + 2K_2b_1^2 + 3K_2K_3b_1^3$ and $\tau_0' = \tau_0 + \tau_{mon} + \tau_{dimer} + \tau_{trimer}$.

Application of Eq. 15 to the light-scattering results leads to the aggregation numbers and second virial coefficients for the higher aggregates (Tables IV–VI).

To apply the corrections suggested by Vrij and Overbeek (17) to this analysis, it is necessary to assume that all low molecular weight aggregates can be taken to be a part of the supporting electrolyte in the same way as the monomers are assumed to be a part of the supporting electrolyte in the treatment of the micellar model (12). This assumption seems justifiable since the small aggregates are of the same charge as the micelles and, therefore, should be excluded effectively from the double layer of

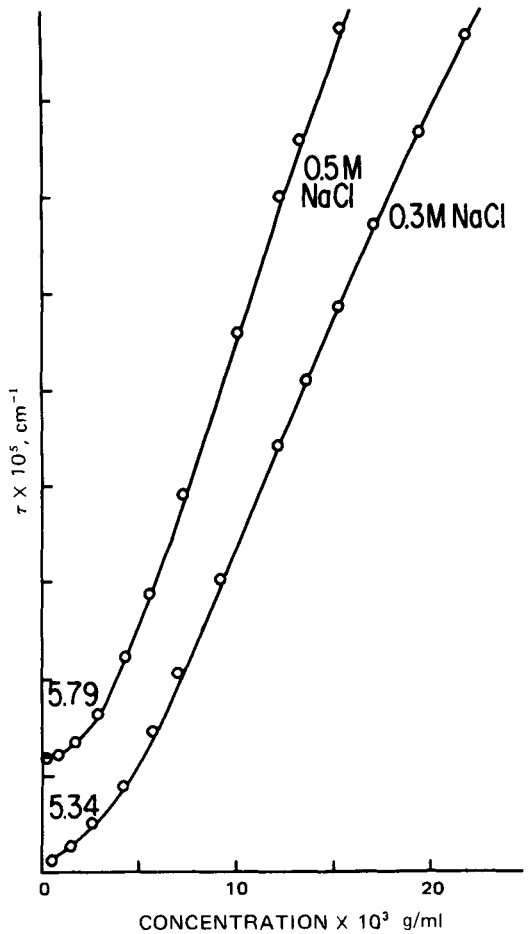

Figure 11—*A plot similar to Fig. 10 for the entire concentration range of 0–25 × 10^{-3} g/ml. The units of the ordinate are the same as in Fig. 1.*

the micelle. This implies that the concentration fluctuations of these aggregates should be independent of micellar fluctuations. Based on this assumption, the true micelle molecular weight was obtained according to Eq. 4. A plot of these data for sodium taurocholate is shown in Fig. 7. The true molecular weights and aggregation numbers obtained for all three bile salts studied are given in Tables IV–VI.

A comparison of the experimental results for sodium taurocholate with the values calculated according to Eqs. 14*b* and 15 is shown in Figs. 8 and 9. For this calculation, the turbidity of the low aggregates was obtained as described earlier. The turbidity of the higher aggregates was obtained in an analogous manner to that used for the high aggregate in the monomer–micelle model. The value of $q\beta_q$ used in fitting the data was 5.5 × 10^{14}. By comparison with Figs. 5 and 6, which give model calculations for the monomer–micelle model, it can be seen that the correlation of this model with the experimental results has improved substantially. In contrast to the monomer–micelle model, no systematic variations exist between the calculated values and the experimental results.

Calculations performed in this manner represent a severe test of the model since average values of K_2, K_3, $q\beta_q$, and B obtained from all four halides were utilized. If, for example, the individual values for each system shown in Table V are utilized, the agreement between the experimental and the calculated curves is much better. This point is further proof of the validity of the assumed model.

Similar correlations between experimental results and calculated values can be obtained for sodium cholate and sodium glycocholate. The values used are shown in Tables IV and VI.

Based on these results, it can be concluded that the self-association of the trihydroxy bile salts in 0.15 *M* sodium halides is best described by a model that assumes the existence of monomers, dimers, trimers, and a higher aggregate containing approximately eight monomeric units. The size of the higher aggregate is not markedly dependent on the bile salt. The only marked difference between the three bile salts appears to be in the value of the dimerization constant, the value for sodium cholate being substantially smaller than that for sodium taurocholate and sodium glycocholate. This result could arise from a decrease in the degree of overlap of the electrical double layers because of the increased length of the side chain of the conjugated bile salts. On the other hand, these effects are not noted in the trimerization constants where charge repulsion would be expected to be greater. This effect may be due to the particular arrangement of the various species in the trimer, which is not known at present.

Effects of Ionic Strength—The effects of ionic strength on the self-association of sodium cholate were studied to a limited extent. For this study, light-scattering curves for sodium cholate in 0.3 and 0.5 *M* sodium chloride were obtained. These results were analyzed according to the methods outlined. However, since data were obtained only in sodium chloride, the more complete analysis according to the method of Vrij and Overbeek (17) cannot be applied. Therefore, the molecular weights and aggregation numbers obtained must be considered to be apparent values, uncorrected for effects due to negative adsorption. The values obtained for K_2, K_3, and the aggregation numbers are shown in Table VII. The calculated values, together with the experimental curves, are shown in Figs. 10 and 11. The agreement between the calculated curves and the experimental values is excellent.

Based on these results, it appears that the pattern of association of sodium cholate is relatively unaffected by changes in the ionic strength of the medium. A comparison of these results with those obtained in 0.15 *M* sodium chloride suggests that the average size of the aggregate might increase slightly with an increase in the ionic strength. This effect is difficult to confirm, however, since the aggregation number is smaller in 0.3 *M* sodium chloride as compared to 0.15 *M* salt. This result may, however, be due to the relatively high values of K_2 and K_3 obtained in 0.3 *M* sodium chloride. This latter result is probably related to experimental difficulties.

REFERENCES

(1) D. M. Small, in "The Bile Acids," vol. 1, P. P. Nair and D. Kritchevsky, Eds., Plenum, New York, N.Y., 1971, chap. 8.

(2) D. M. Small, *Adv. Chem. Ser.*, **84**, 31 (1968).

(3) P. Ekwall, K. Fontell, and A. Sten, *Proc. Int. Congr. Surf. Act., 2nd*, **1957**, 397.

(4) K. Fontell, *Kolloid Z.-Z. Polym.*, **244**, 246 (1971).

(5) *Ibid.*, **244**, 253 (1971).

(6) *Ibid.*, **250**, 333 (1972).

(7) P. Mukerjee and J. R. Cardinal, *J. Pharm. Sci.*, **65**, 882 (1976).

(8) L. B. Vitello, Ph.D. thesis, Clarkson College of Technology, Potsdam, N.Y., 1973.

(9) A. F. Hofmann, *Acta Chem. Scand.*, **17**, 173 (1963).

(10) L. Lack, F. O. Dorrity, Jr., T. Walker, and G. D. Singletary, *J. Lipid Res.*, **14**, 367 (1973).

(11) R. H. Schipmann and E. Farber, *J. Polym. Sci.*, **B1**, 65 (1963).

(12) H. F. Huisman, *Konik. Ned. Akad. Wetenschap. Proc. Ser.*, **B67**, 367, 376, 388, 407 (1964).

(13) D. J. Coumou, *J. Colloid Sci.*, **15**, 408 (1960).

(14) J. P. Kratohvil and H. T. DelliColli, *Can. J. Biochem.*, **46**, 945 (1968).

(15) P. DeMoerloose and R. Ruyssen, *J. Pharm. Belg.*, **14**, 95 (1959).

(16) P. Debye, *J. Phys. Colloid Chem.*, **51**, 18 (1947).

(17) A. Vrij and J. T. G. Overbeek, *J. Colloid Sci.*, **17**, 570 (1962).

(18) M. C. Carey and D. M. Small, *J. Colloid Interface Sci.*, **31**, 382 (1969).

(19) T. Furasawa, *Fukuoka Acta Med.*, **53**, 124 (1962).

(20) R. F. Steiner, *Arch. Biochem. Biophys.*, **39**, 333 (1952).

(21) D. Attwood and O. K. Udeala, *J. Phys. Chem.*, **79**, 889 (1975).

(22) D. Attwood and O. K. Udeala, *J. Pharm. Sci.*, **65**, 1053 (1976).

(23) K. J. Mysels and L. H. Princen, *J. Phys. Chem.*, **63**, 1649 (1959).

(24) P. Mukerjee, K. J. Mysels, and C. I. Dulin, *ibid.*, **62**, 1390 (1958).

(25) P. Mukerjee, *J. Pharm. Sci.*, **63**, 972 (1974).

ACKNOWLEDGMENTS

Abstracted in part from a dissertation submitted by Y. Chang to the University of Utah in partial fulfillment of the Doctor of Philosophy degree requirements.

Financial support by the University of Utah Research Committee is gratefully acknowledged.